sciendo

Acta Materialia Transylvanica 5/1. (2022) 1–5.
DOI: Hungarian: https://doi.org/10.33923/amt-2022-01-01
English: https://doi.org/10.33924/amt-2022-01-01

ACTA MATERIALIA TRANSYLVANICA

Simulation of CuE Copper Alloy in a Closed-Die Multi-Axial Forging Tool

Tamás BÍRÓ,[1] Zsombor JUHÁSZ,[2] József Bálint RENKÓ[3]

[1] *Budapest University of Technology and Economics, Department of Materials Science and Engineering, Faculty of Mechanical Engineering, Budapest, Hungary, biro.tamas@edu.bme.hu*

[2] *Budapest University of Technology and Economics, Department of Materials Science and Engineering, Faculty of Mechanical Engineering, Budapest, Hungary, juhasz.zsombor@edu.bme.hu*

[3] *Budapest University of Technology and Economics, Department of Materials Science and Engineering, Faculty of Mechanical Engineering, Budapest, Hungary, renko.jozsef@edu.bme.hu*

Abstract

Two-way multi-axial forging was performed on a newly designed closed-die forging tool. The tool was operated on an MTS 810 material testing system. The connected computer recorded force and crosshead displacement as a function of time during operation. The sample material of the four-step forging experiment was CuE copper alloy. The plastic deformation was 0.8 per step, thus the rate of cumulative equivalent plastic strain was 3.2 by the end of the process. The speed of movement of the active tools during the whole test was 2 mm/min. Finite element simulation was performed with QForm3D software to investigate the force conditions of the process. The necessary flow curve was determined by Watts-Ford test. The force-displacement curves of the physical simulation were compared with the results of the finite element modeling.

Keywords: *multi-axial forging, finite element modeling, Watts-Ford test.*

1. Introduction

In recent years ultrafine and nanograined materials have become very popular in materials science[1]. This is due to their more favourable mechanical properties compared to the same quality coarse-grained materials. Ultrafine grain structure can result in increased strength, higher fatigue limits, and increased toughness [2–3]. There are several methods to create these materials [4–6]. Those that apply significant shear stress on the material are called severe plastic deformation (SPD) processes [7–9]. Multi-axial forging is one of these methods [10–11].

Earlier a newly designed, closed-die forging tool was developed to investigate the mechanical properties of materials that can be produced by multi-axial forging. Our aim was to investigate the force history of a four-step forming with this new tool. Additionally, the previously implemented physical simulation was recreated with finite element modeling. Thus, we could compare the recorded force-displacement curves and draw conclusions about the reliability of the finite element model.

2. Experimental

2.1. Material

In order to keep the tool loads at a controllable level, a suitably soft material had to be selected as workpiece. Thus, the chosen material was industrial grade copper. The chemical composition of the CuE material was measured by EDAX Z2 type SEM-EDS system, but it could not detect a significant amount of impurities. The workpiece nominal dimensions were $10 \times 10 \times 20$ mm. This geometry was machined from block material. To reach the softest state of the material, the workpiece was placed in an oven preheated to 950 °C, and after 15 minutes of holding at this temperature, it was put into cold water. This heat treatment eliminated the effects of aging and the unknown deformation history prior to the tests [12].

2.2. Equipment

The tool used for physical simulations is composed of three main parts as shown in Figure 1. lThe first part is the center block, where the forging takes place. The second part is the tool housing, which frames the other components and ensures the relative position of the individual parts to one another.

Finally, linear actuators are included to provide the tool movements required for forming. The four self-moving stamps are connected by the tool housing. Thus, the stamps facing each other always move together, but with a maximum displacement of no more than 5-5 mm.

An MTS 810 universal material testing system was used to implement the necessary tool movements and to record the displacement and force data as a function of time. The maximal measuring limit of the equipment was 250 kN. During forging, the movement speed of the crosshead was 4 mm/min, which results a 2 mm/min movement speed for each tool.

To minimize tool loads, the friction had to be reduced. To achieve this, proper lubrication of the workpiece and the forming cavity was essential [13]. Surfaces directly contacting the workpiece were coated with zinc stearate paste prior to testing. Due to the closed nature of the die cavity, the cover plate must be temporarily removed for lubrication and insertion of the workpiece, and then reattached before the first forming step.

At the end of the current forging step, the tool returns to its initial position. The geometry of the workpiece is the same as the initial one, but rotated 90 ° in space. Due to the symmetrical design of the tool, with a 90 ° rotation, the relative position of the tool and the workpiece to the MTS system can be reset without opening the tool forming cavity. After rotating the whole tool, the next forming step follows.

2.3. Physical simulations

During the physical simulations four consecutive forming steps were performed, while the displacement of the crosshead and the force were recorded as the function of time. Figure 2 shows the first two forging steps, as they are representative of the whole cyclic process.

Assuming a plane strain state, the logarithmic deformation of the workpiece is approximately 0.80. (1)

$$\varphi = \frac{2}{\sqrt{3}} \cdot ln\left(\frac{H}{h}\right) = \frac{2}{\sqrt{3}} \cdot ln\left(\frac{20}{10}\right) = 0.80 \qquad (1)$$

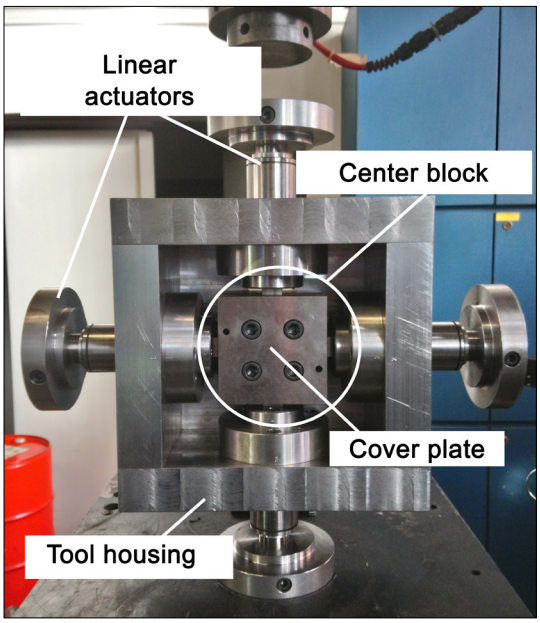

Figure 1. *General construction and main parts of the used closed-die multi-axial forging tool*

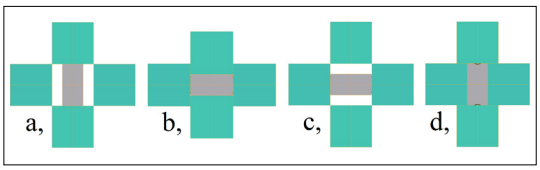

Figure 2. *Schematic figure of two consecutive forming steps while maintaining the position of the workpiece (gray). Starting position (a), final state of the first forging step (b), tools move back to their initial position (c), end of the second forging step (d)*

where φ is the plastic strain, H is the initial height of the workpiece and h is the workpiece height measured at the end of the forging step [14].

The cumulative plastic deformation (φ_{kum}) can accordingly be calculated as the sum of the plastic strains achieved in each forging step (2). In the 4-step forming process presented in the current study, its value is 3.2.

$$\varphi_{kum} = 4 \cdot \frac{2}{\sqrt{3}} \cdot ln\left(\frac{20}{10}\right) = 3.2 \qquad (2)$$

2.4. Finite element modeling

A finite element model was developed to reproduce and analyse the multi-axial forging process. To create the finite element model, QForm3D software was used. 3D models can give more accurate

results of the process than 2D models, but their computation requirements are significantly higher. Due to the arrangement of the tools and the symmetry of their movements, it is sufficient to use an eighth model, which can reduce the maximum number of elements and, consequently, the required computational time. The nominal dimensions of the tool and the workpiece were used to create the necessary geometry, and the displacement-time data measured during the physical simulations were used for the tool movements [15]. The assembled model is shown in Figure 3.

The finite element mesh was automatically created by the software. Additionally, the workpiece was remeshed in each calculation step. Mesh refining was also applied in the contact area between the workpiece and the tool. For the whole process tetragonal elements were used. Their initial number was 29069, but by the end of the simulation, this had increased to 33748 due to continuous mesh refinement.

The flow curve used in the calculations was measured by Watts-Ford test on a specimen prepared under the same conditions as the workpiece [16]. It is important to point out that the maximum plastic strain here was only 2.97, so the stress-strain curve beyond this value was generated by the program based on the fitted curve (Figure 4).

3. Results and discussion

The change of force as a function of displacement measured during the physical simulations is shown in Figure 5.

Within each forming step, the force increased monotonically, and the force requirement of each forming step increased with the number of forming steps. At the end of the first three steps, the increase in force was nearly the same at 10 kN. Thereafter, the increment in force was reduced, and the force of the fourth step did not change significantly compared to the previous step. The dislocation density of the softened copper is presumably no longer increasing after the third forming step to such an extent that it causes a significant increase in the force [17].

The force-displacement curves of the finite element model show a similar trend with the results of the physical simulation (Figure 6).

As the forming steps progress, the force also increases step by step, and maintains its monotonous nature within a given step. In contrast to the

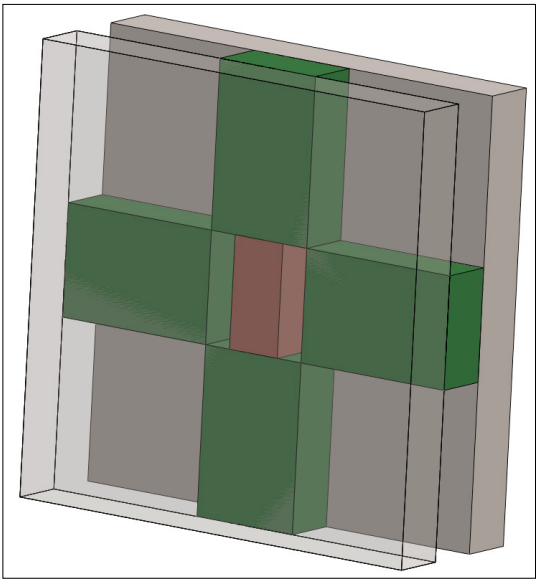

Figure 3. *The 3D models used in the simulation.*

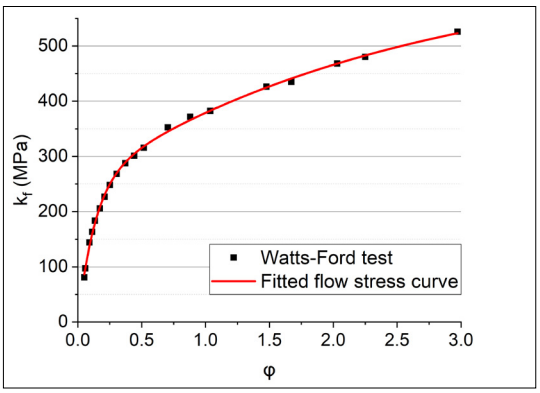

Figure 4. *Watts–Ford test result and flow curve fitted to the data.*

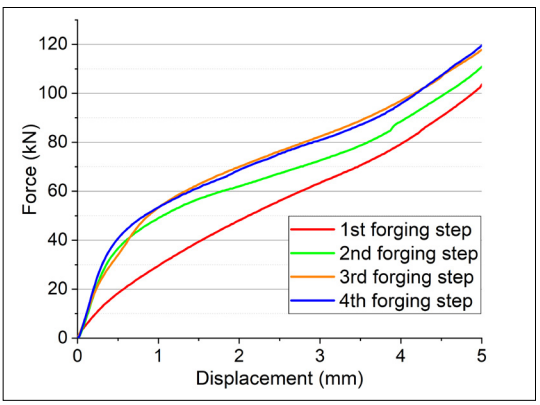

Figure 5. *Force-displacement curves obtained by the physical simulation of multi-axial forging.*

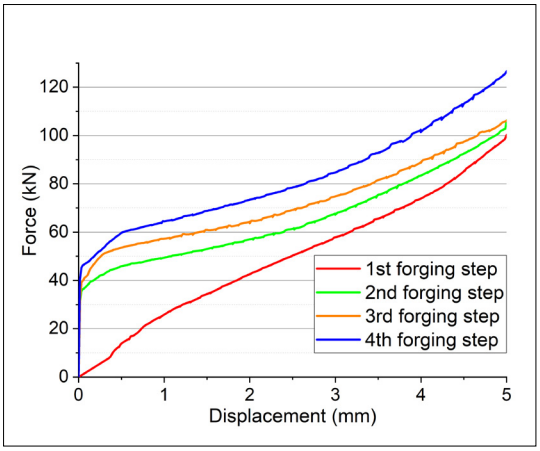

Figure 6. *Force-displacement curves obtained by finite element modeling.*

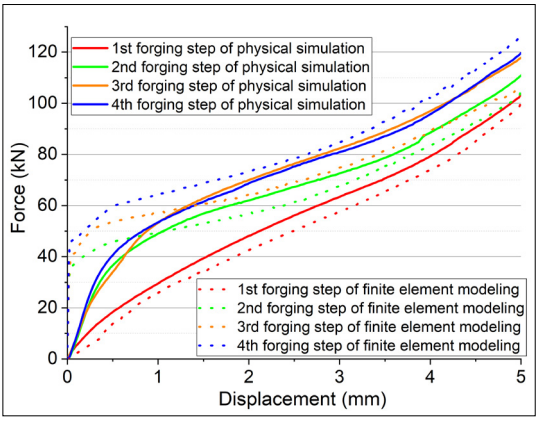

Figure 7. *Comparison of force-displacement curves resulting from physical simulation and finite element modeling.*

physical simulation, the force increase at the end of the first three steps is only about 5 kN. By the end of the fourth step, the force shows a drastic increase. The reason for this is presumably that the flow stress curve recorded by the Watts-Ford test was not measured over the entire test range, and in the second half of the fourth step, the fitted curve presumably rose steeper than reality.

By fitting the curves of the physical and finite element simulations to each other, for a given forging step the curve of the physical simulation is located slightly below the curve of the finite element model (**Figure 7**).

An exception to this trend is the curve for the fourth forging step, where the force values obtained with the finite element model jump drastically. This can be traced back to several reasons. On one hand, it can be assumed that the fitted flow-stress curve does not flatten after leaving the studied deformation range of Watts-Ford test as it would in reality. On the other hand, the difference may also be related to the deformation history of the workpiece. The tests were preceded by a softening heat treatment, so the deformation of the material could start from an almost isotropic state and could be transformed into an anisotropic structure during forging. The effect of this on the macroscopic properties presumably reached the extent that it could be detected in the third and fourth forming steps.

4. Conclusions

We performed successful experiments with a closed-die multi-axial forging tool. The four forming steps were performed by rotating the tool 90° after each step without opening the die cavity. Examining the obtained force-displacement curves, the measured force increased step by step. These characteristics were also supported by the finite element model of the process. The differences in the finite element model, especially those experienced during the fourth forming step were caused by the differences in the test ranges of the physical simulation and the Watts-Ford test. The finite element model was able to approximate reality, but to improve its accuracy it is necessary to refine the applied material model.

Acknowledgement

Supported by the ÚNKP-21-2-I-BME-218 New National Excellence Program of the Ministry for Innovation and Technology from the source of the National Research, Development and Innovation Fund.
The publication of the work reported herein has been supported by GMKA at BME.

References

[1] Huang Y., Langdon T. G.: *Advances in ultrafine-grained materials*. Materials Today 16/3. (2013) 85–93. https://doi.org/10.1016/j.mattod.2013.03.004
[2] Valiev R. Z., Islamgaliev R. K., Alexandrov I. V.: *Bulk nanostructured materials from severe plastic deformation.* Progress in Materials Science, 45. (2000) 103–189. https://doi.org/10.1016/S0079-6425(99)00007-9
[3] Langdon T. G.: *The principles of grain refinement in equal-channel angular pressing.* Materials Science and Engineerig A, 462. (2007) 3–11. https://doi.org/10.1016/j.msea.2006.02.473
[4] Segal V. M., Reznikov V. I., Drobyshevkij A. E. Kopylov V. I.: *Plastic Working of Metals by Simple Shear*. Russian Metallurgy, 1. (1981) 99–105.

[5] Toth L. S., Vu V. Q., Dhinwal S. S., Zhao Y., Massion R., Chen C., Davis C. F., Lowe T. C.: *The mechanics of High Pressure Compressive Shearing with application to ARMCO® steel.* Materials Characterization, 154. (2019) 127–137. https://doi.org/10.1016/j.matchar.2019.05.039

[6] Szabó P. J., Bereczki P., Verő B.: *The Effect of Multiaxial Forging on the Grain Refinement of Low Alloyed Steel.* Periodica Polytechnica Mechanical Engineering, 55/1. (2011) 63–66. https://doi.org/10.3311/pp.me.2011-1.09

[7] Huang Y., Langdon T. G.: *Advances in ultrafine-grained materials.* Materials Today, 16/3. (2013) 85–93. https://doi.org/10.1016/j.mattod.2013.03.004

[8] Jin X., Chena S., Rong L.: *Microstructure modification and mechanical property improvement of reduced activation ferritic/martensitic steel by severe plastic deformation.* Materials Science & Engineering A, 712. (2018) 97–107. https://doi.org/10.1016/j.msea.2017.11.095

[9] Sadasivan N., Balasubramanian M.: *Severe plastic deformation of tubular materials – Process methodology and its influence on mechanical properties – A review.* Materials Today: Proceedings, 46. (2021) 3460–3468. https://doi.org/10.1016/j.matpr.2020.11.859

[10] Trivedi P., Nune K. C., Misra R. D. K., Goel S., Jayganthan R., Srinivasan A.: *Grain refinement to submicron regime in multiaxial forged Mg-2Zn2Gd alloy and relationship to mechanical properties.* Material Science and Engineering: A, 668. (2016) 59–65. https://doi.org/10.1016/j.msea.2016.05.050

[11] Naser T. S. B., Krállics G.: *The effect of multiple forging and cold rolling on bending and tensile behavior of Al 7075 alloy.* Materials Science Forum, 729. (2012) 464–469. http://doi.org/10.4028/www.scientific.net/MSF.729.464

[12] Chen X., Zhao G., Xu X., Wang Y.: *Effects of heat treatment on the microstructure, texture and mechanical property anisotropy of extruded 2196 Al Cu Li alloy.* Journal of Alloys and Compounds, 862. (2021) 158102. https://doi.org/10.1016/j.jallcom.2020.158102

[13] Wilson W. R. D.: *Friction and Lubrication in Bulk Metal-Forming Processes*. Journal of Applied Metalworking, 1. (1978) 7–19.

[14] Valberg H. S.: *Applied Metal Forming*. Cambridge University Press, (2010) 53–76.

[15] Zienkiewicz O. C., Taylor R. L.: *The Finite Element Method. Solid Mechanics.* 5. kiadás. Butterworth-Heinemann, Oxford, 2000. 1–21.

[16] Watts A.B., Ford H.: *On the Basic Yield Stress for a Metal.* Proceedings of the Institution of Mechanical Engineers, 169/1. (1955) 1141–1156.

[17] Shakhova I., Yanushkevich Z., Fedorova I., Belyakov A., Kaibyshev R.: Grain refiment in a Cu Cr Zr alloy during multidirectional forging. Material Science and Engineering, 606. (2014) 380–389.